Li, Zhan-dong et al.

Article

Experimental study on growth characteristics of pore-scale methane hydrate

Energy Reports

Provided in Cooperation with:
Elsevier

Suggested Citation: Li, Zhan-dong et al. (2020) : Experimental study on growth characteristics of pore-scale methane hydrate, Energy Reports, ISSN 2352-4847, Elsevier, Amsterdam, Vol. 6, pp. 933-943,
https://doi.org/10.1016/j.egyr.2020.04.017

Energy Reports 6 (2020) 933–943

Contents lists available at ScienceDirect

Energy Reports

journal homepage: www.elsevier.com/locate/egyr

Research paper

Experimental study on growth characteristics of pore-scale methane hydrate

Zhan-dong Li [a,b,c,*], Xin Tian [c], Zhong Li [d], Jin-ze Xu [e,**], Hai-xiang Zhang [a], Dian-ju Wang [a]

[a] Heilongjiang Key Laboratory of Gas Hydrate Efficient Development, Heilongjiang Daqing 163318, China
[b] ColleGe of Offshore Oil and Gas Engineering, Northeast Petroleum University, Heilongjiang Daqing 163318, China
[c] College of Petroleum Engineering Institute, Northeast Petroleum University, Heilongjiang Daqing 163318, China
[d] Zhanjiang Branch of CNOOC Limited, Guangdong Zhanjiang 524057, China
[e] Department of Chemical and Petroleum Engineering, University of Calgary, Calgary, AB T2N 1N4, Canada

ARTICLE INFO

Article history:
Received 1 February 2020
Received in revised form 3 April 2020
Accepted 8 April 2020
Available online xxxx

Keywords:
Gas hydrates
Nucleation and growth
Methane
Visualization
Pore scale
Heterogeneous nucleation

ABSTRACT

In order to study the behavioral characteristics of the pore-scale hydrate formation, this experiment employs a high-pressure-resistant visible model in an etched glass plate to study the pore-scale methane hydrate formation and reveal its growth law s in porous media. The experiment shows that the evolution of natural gas hydrates is divided into three periods, namely, the instability period of gas–liquid dissolution, the hydrate growth period, and the hydrate formation period. The hydrate growth process accelerates when pressure increases. The increase in temperature yields a random trend.

The hydrate growth period has three substages: the gas–liquid cluster and nucleation stage, the gas–liquid film formation and accretion stage, and the deposition and crystallization stage. The hydrate growth laws are drawn as follow: (1) The nucleation characteristics of the gas hydrate directly determine the hydrate's spatial distribution in the pores. The heterogeneous nucleation is more likely to occur. (2) The spatiotemporal growth of the hydrates is an interaction of two kinds of transformations in the porous media, namely, the transformation from the disordered to the ordered, and the transformation from the hydrophobic to the hydrophilic. In the early stage, the gas–liquid contact appears to be hydrophobic, and the gas–liquid dissolution process shows a repeated disorder. In the later stage, the hydrate begins to be "hydrophilic", which means it follows the existing hydrate interface to grow orderly into the depth of the pores. (3) The geometric distribution of the pore structure can change the spatial structure of the water molecules' growth, which leads the hydrate to distribute with a geometric anisotropy. The research results are aimed to provide a theoretical basis for the exploitation and optimization of marine natural gas hydrates.

1. Introduction

With unique advantages of small pollution, vast reserves, wide distribution and high energy density, Natural Gas Hydrate (NGH), or hydrates for short, are known as the commanding height for the global energy development in the future (Sloan, 1998) and have attracted worldwide attention. It is estimated that the organic carbon reserves in the hydrates worldwide are equivalent to two times the world's proved fossil fuels (including coal, oil, and natural gas). Because of these advantages, Mallik plan started in 2002, which was the joint contribution of 8 agencies in 5 countries. Since Mallik plan carried out hydrate trial production in the permafrost zone of Mackenzie Delta in Canada, at least 7 major hydrate trial production events had happened by the end of 2017, with rich practical experience being accumulated in natural gas hydrate trial production. However, after years of general survey and trial production, the fundamental research on hydrate is still far from the demand for commercial mining.

Natural gas hydrate is a mixture (National Energy Technology Laboratory of U.S. Department of Energy, 1999-2016) generated under certain temperature and pressure conditions. The accumulation of hydrates is based on the formation of hydrates. It is still an elusive and essential goal to describe the microscopic mechanism of hydrate formation comprehensively. The generation of hydrate is a complex multi-component transportation process. In particular, the hydrate nucleation is a rare event, which requires observation and analysis at microscale. At present, the observation methods for the induction time of hydrate nucleation mainly include the pressure variation method, the temperature variation method, and the eye observation method. The pressure variation method and the temperature variation method are based on

* Corresponding author at: College of Petroleum Engineering Institute, Northeast Petroleum University, Heilongjiang Daqing 163318, China.
** Corresponding author.
E-mail addresses: lzd@nepu.edu.cn (Z.-d. Li), jinzxu@ucalgary.ca (J.-z. Xu).

https://doi.org/10.1016/j.egyr.2020.04.017

quantitative measurements during the hydrate generation process, but the data recording methods are different. The pressure variation method is to inject gas into the reactor and maintain a specific pressure in the reactor, then record the pressure change over time at a constant temperature. This method neglects the temperature variation during the hydrate generation.

In terms of the temperature variation method, when hydrate formation is happening at a low temperature, this exothermic reaction will release a large amount of heat, causing the system temperature to rise immediately. Therefore, the hydrate nucleation may not be sufficiently representative based on the data of temperature change over time, especially in the understanding of pore distribution. The eye observation method is to observe the interior of the reactor through a window. When the interior begins to be turbid, it can be determined that the hydrate nucleation has begun. However, experimental devices have limitations. Nuclear magnetic resonance is a static measurement, which reflects the hydrate formation and distribution in the pore spaces comprehensively based on the relaxation time of hydrogen nuclei in the pore fluid. However, it cannot measure the data related to the throat. Therefore, every method mentioned above reflects only one aspect of the hydrate nucleation process. It is significant and also challenging to combine these methods effectively for the comprehensive evaluation of hydrate formation.

The spatial distribution of hydrate in the pores is closely related to the nucleation characteristics of gas hydrate. For instance, Matthew et al. studied the nucleation and formation mechanism of spontaneous methane hydrate from the perspective of molecular dynamics simulation (Wan et al., 0000). Kleinberg et al. found that the hydrate formation efficiency was variable (Lu et al., 2011). Tohidi et al. used artificial glass model to simulate the micro pores, and found that the hydrate was formed in the center of the pores instead on the surface of the particles (Zunzhao et al., 2007). Xue used the etching method to create an artificial microchannel model on the glass plate, and illustrated the formation condition of the hydrate's occurrence structure from the perspective of nucleation kinetics (Ota et al., 2005). Katsuki et al. Used glass channels and found that gas phase of methane is not formed on the hydrate's crystal surface during the dissociation process (Xu and Li, 2015).

However, the academia have not come to a clear definition of the hydrate nucleation process. Due to the limitations of experimental methods, the nucleation process is still inexplainable on the micro-level. Several vital challenges remain regarding the hydrate formation and distribution mechanism in the sediment. Firstly, there is a gap between the regular grid and the real condition of the underground reservoir, which makes the microstructure of the hydrate formation has an unclear evolution. Secondly, the control factors in the hydrate nucleation period are not apparent. Thirdly, in porous media, the order–disorder transition happened in the hydrate formation, and the hydrophobic-hydrophilic interaction should be further studied. Therefore, in order to explore the micro-formation mechanism of hydrate at a pore-scale, based on the high-pressure-resistant visual model made by etching method on the glass plate, this experiment can comprehensively describe the micro-formation mechanism of hydrate in porous media after an observation of the hydrate crystal formation in porous media through a microscope. In other words, this experiment is to describe the hydrate crystal formation process in the pores and throat, analyze the distribution and size of hydrate in micro-porous structure, find out the time-varying characteristics during the hydrate formation, and conclude the dynamic process of hydrate nucleation and the controlling factors. The research results are aimed to provide data and theoretical basis for the selection and optimization of marine gas hydrate exploitation methods.

2. Experimental equipment and research approach

2.1. Experimental equipment

This experiment uses a self-made experimental device for the hydrate formation and decomposition in a micro-scale (Fig. 1). The device mainly consists of four parts: the air induction system, the temperature control system, the simulation system for the hydrate formation and decomposition, and the monitoring system. Through a built-in transparent lithographic glass, the reactor is visible, which is achieved by welding one quartz glass plate to another, and carving a microchannel like the core pore throat on the quartz glass plate. The reactor is sealed at both ends, and the inner wall is threaded and fitted with an O-ring. The two ends of the reactor are stainless-steel cylinders sealed by hexagonal screws. Both the length and the width of the built-in lithographic glass are 10 cm, with a thickness of 1 cm. The reactor shall be kept dry at a constant temperature before the experiment. The hydrate synthesis and decomposition parameters are shown in Table 1. The two ends of the reactor are fitted with an inlet valve or an outlet valve. Pressure sensors are installed respectively on both ends. Resistance test points are set to monitor the change during the hydrate synthesis process, with one setting at the inlet end, one at the middle part, and two at the outlet end. The Gas flowmeters are installed at the inlet and outlet of the reactor.

A temperature sensor with an error of ± 1 °C and a control range of −40-100 °C is equipped in the pipeline of the temperature control system. A pressure sensor with an accuracy of 0.01 MPa and a range of 0–40 MPa is equipped inside the reactor. The pressure sensor and the temperature sensor are to monitor the pressure change and temperature change at the reactor's inlet and outlet. Two gas flowmeters with an accuracy of 0.001ml and a response time of no more than 0.5s are set respectively at the gas inlet and outlet of the reactor, to measure the gas injection amount, the gas output amount, and the gas flow rate. Data collected in this experiment include the gas injection volume, liquid injection volume, gas injection velocity, liquid injection velocity and data related to hydrate formation. The monitoring system will output the videos collected by the microscope to the computer. The incubator and the reactor have different temperatures during the experiment, leading to a high degree of heat exchange between the reactor and the external environment. Therefore, each experiment group should be kept at a constant temperature for more than 1 h before the data is recorded. The experimental environment is approximately isolated from and the external environment during the whole reaction process.

This experiment uses CH4-produced methane gas with a purity of 99% and laboratory-made distilled water and NaCl. After screening, the lithographic glass used in this experiment has different pore diameters, whose pore composition and characteristics are similar to the rock stratum where the natural gas hydrate is reserved. Both the length and the width of the lithographic glass are 10 cm. The thickness is 1 cm.

2.2. Research approach

Heat the incubator to 40 °C, then turn on the incubator and heat for 15-20 min to keep the incubator dry. Fix the reactor, which is equipped with the lithographic glass, in the incubator, connect the water injection valve and the gas injection valve, install the ring LED light source under the lithographic glass, and install the electron microscope over the lithographic glass. Turn on the video collector, and adjust the electron microscope to make the video clear. Turn off the incubator and collect the video of the reaction process. Then open the water injection valve to inject water into the lithographic glass, lower the temperature of

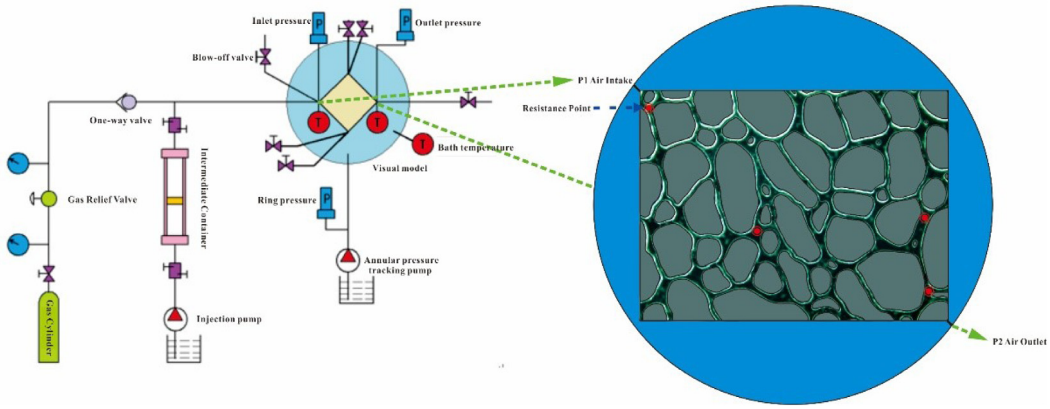

Fig. 1. The micro-scale system of gas hydrate formation.

the incubator to 3 °C, and keep the temperature constant at 3 °C for 2 h, which can effectively reduce the temperature difference between the incubator and the lithographic glass. Open the gas cylinder to inject methane into the ring pressure device, and then inject methane into the lithographic glass through the ring pressure device, which can avoid the problems that the gas flow rate is unstable, and the gas injection volume is unmeasurable during the gas injection process. When the pressure inside the lithographic glass reaches the preset pressure, turn off the ring pressure device.

During the experiment, the temperature of the incubator is adjusted several times. It is kept at 3 °C for 2 h, and then lowered by 0.1 °C and kept for 1 h until the hydrate synthesis finishes. After the formation of hydrate, the temperature is lowered to 0 °C, and kept at 0 °C for more than 10 h. The time duration for the hydrate formation is about 1080 s. When the pressure is stable at about 10 MPa for a long time (more than 10 h), it can be considered that the hydrate is stable.

2.3. Data analysis

Data collected in this experiment are mainly consist of the injection gas volume, the temperature of the porous media, the pressure, the resistivity and the gas-phase velocity. The data is input to the computer through the data acquisition system. The monitoring and data collection during the experiment are accomplished mainly through two methods, video collection and data acquisition at the measuring points. To be specific, observe the hydrate formation and variation in the porous media through videos, and record the parameters of temperature, pressure, resistivity and gas flow to reflect the progress of the decomposition experiment. With the help of scientific analysis, the understanding of the law of NGH formation can be further deepened. Fig. 2a-c records the resistivity, temperature-pressure and the growth rate curve over time of this methane hydrate formation experiment. These figures show the curves of resistivity, temperature and pressure vary with time. After the experiment, calculate the water saturation of the samples.

Hydrate formation happens in the form of the methane gas entering the aqueous phase, so the hydrate saturation can be calculated indirectly by calculating the gas consumption at the time. Use the gas equation of state to calculate the methane gas consumption, in other words, the difference value between the methane gas amount before the reaction n_1 and the residual methane gas amount after the reaction n_2:

Table 1
Parameters during the hydrate formation process.

Time /s	Temperature /K	Pressure /Mpa	Resistivity /(Ω*m)	Saturation /%
0	275.0	0	3.691	0
100	275.6	2.2	3.989	0
200	275.4	4.9	4.493	0
300	275.7	9.1	3.021	10.06
400	275.9	10.1	3.493	21.80
500	276.8	10.2	3.563	33.69
600	277.1	10.4	3.634	42.70
700	277.4	10.3	3.787	55.54
800	277.6	10.4	4.876	61.98
900	278.2	10.6	5.948	73.32
1000	278.9	10.7	6.763	82.17

$$\begin{cases} n_1 = \dfrac{(PV)_1}{R\,(ZT)_1} \\ n_2 = \dfrac{(PV)_2}{R\,(ZT)_2} \\ n_{\text{※}} = n_1 - n_2 \end{cases} \tag{1}$$

In the above formula,

—the amount of methane injected before the reaction. Unit: Mol

—the residual methane gas amount after the reaction. Unit: Mol

—the amount of methane consumed in hydrate formation. Unit: Mol

P—the pressure at any time inside the lithographic glass. Unit: PA

V—the volume of gaseous methane. Unit: m^3

R—the gas constant. R= 8.314

T—the temperature at any time in the lithographic glass. Unit: K

Z—the compression factor

In the above formula, P, V and T can be measured through experiment. However, the conventional compression factor is not suitable for the environment with high pressure and low temperature, so the compression factor should be calculated by the BWRS equation.

$$\begin{aligned} P = {} & \rho RT + \left(B_0 RT - A_0 - \frac{C_0}{T^2} + \frac{D_0}{T^3} - \frac{E_0}{T^4}\right) \\ & + \left(bRT - a - \frac{d}{T}\right)\rho^3 + a\left(a + \frac{d}{T}\right)\rho^6 \\ & + \frac{C\rho^3}{T^3}\left(1 + \gamma\rho^2\right) e^{\left(-\gamma\rho^2\right)} \end{aligned} \tag{2}$$

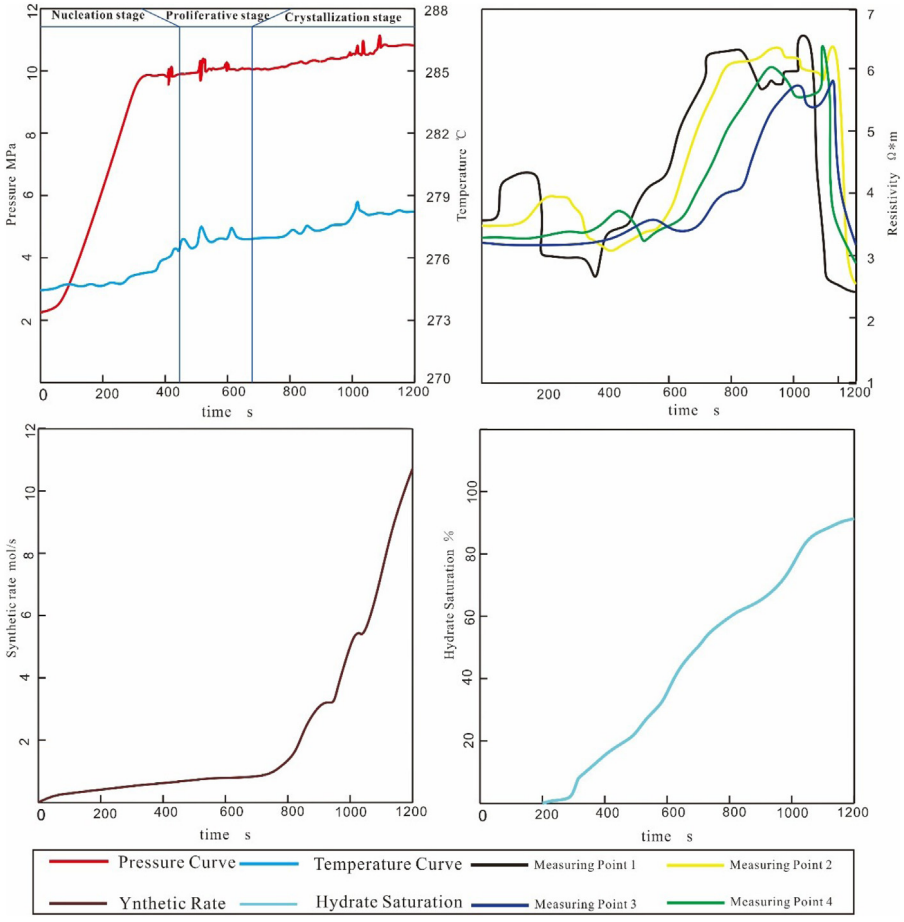

Fig. 2. Hydrate parameter variation curve.

Parameters a, b, c, d, α, γ, A_0, B_0, C_0, D_0, E_0 in the above formula can be calculated by the following formula.

$$\begin{cases} \rho_{ci}B_{oi} = A_1 + B_1 w_i \\ \frac{\rho_{ci}A_{oi}}{RT_{ci}} = A_2 + B_2 w_i \\ \frac{\rho_{ci}C_{oi}}{RT_{ci}^3} = A_3 + B_3 w_i \\ \rho_{ci}^2\gamma_i = A_4 + B_4 w_i \\ \rho_{ci}^2 b_i = A_5 + B_5 w_i \\ \frac{\rho_{ci}^2 a_i}{RT_{ci}} = A_6 + B_6 w_i \\ \rho_{ci}^3 b_i = A_7 + B_7 w_i \\ \frac{\rho_{ci}^3 c_i}{RT_{ci}^3} = A_8 + B_8 w_i \\ \frac{\rho_{ci}D_{oi}}{RT_{ci}^4} = A_9 + B_9 w_i \\ \frac{\rho_{ci}^2 d_i}{RT_{ci}^2} = A_{10} + B_{10} w_i \\ \frac{\rho_{ci}E_{oi}}{RT_{ci}^5} = A_{11} + B_{11} w_i e^{(-3.8 w_i)} \end{cases} \quad (3)$$

In the above formula, ——can be obtained from Table 2, Parameters of the BWRS Equation (Zhou et al., 2008). is the critical temperature of methane. 190.7 K. is the critical density of methane. 10.1 kmol/m^3. is the acentric factor. 0.013.

Rewrite the BWRS equation into a function equation:

$$F_\rho = \rho RT + \left(B_0 RT - A_0 - \frac{C_0}{T^2} + \frac{D_0}{T^3} - \frac{E_0}{T^4}\right) + \left(bRT - a - \frac{d}{T}\right)\rho^3 + a\left(a + \frac{d}{T}\right)\rho^6 + \frac{C\rho^3}{T^3}\left(1 + \gamma\rho^2\right)e^{\left(-\gamma\rho^2\right)} \quad (4)$$

Suppose that when $F_\rho = 0$, then calculate ρ_1 through iterative computations:

$$\rho_{k+1} = \frac{\rho_{k-1}F_{(\rho_k)} - \rho_k F_{(\rho_{k-1})}}{F_{(\rho_k)} - F_{(\rho_{k-1})}} \quad (5)$$

The value of ρ can be obtained by the above formula. Then ρ is substituted into the calculation formula for the compression factor:

$$Z = \frac{p}{\rho RT} \quad (6)$$

The compression factor Z can be obtained by the above formula.

Then Z is substituted into the gas state equation, through which the methane consumption at any time in the lithographic glass can be solved, which equals to the hydrate saturation (Table 1). Fig. 2d is the time curve of the water saturation change of the hydrate after calculation.

3. Experiment results and discussion

3.1. The time-varying characteristics of the hydrate formation

The process of hydrate formation starts from the time point when the methane gas dissolves in aqueous solution. It enters

Table 2
Parameters of the BWRS equation.

Parameter	Value	Parameter	Value	Parameter	Value	Parameter	Value
A_1	0.44369	A_7	0.07052	B_1	0.11545	B_7	−0.0444
A_2	1.28438	A_8	0.50409	B_2	−0.9207	B_8	1.32245
A_3	0.35631	A_9	0.03075	B_3	1.70871	B_9	0.17943
A_4	0.54498	A_{10}	0.07328	B_4	−0.2709	B_{10}	0.46350
A_5	0.52863	A_{11}	0.00645	B_5	0.34962	B_{11}	−0.0221
A_6	0.48401			B_6	0.75413		

the nucleation-crystallization period when ice nuclei larger than the critical size appear in the aqueous solution, then finally forms the hydrate in the macro sense. According to the time sequence, the spontaneous growth and the evolution of hydrate can be divided into three periods, namely, the instability period of gas–liquid dissolution, the hydrate growth period, and the hydrate formation period. The nucleation and spontaneous growth of hydrate are the main focus of this study, which occur in the hydrate growth period and will be analyzed in detail in the next section. Fig. 3 is an evolution diagram that describes the occurrence states at different times during the hydrate growth process. Fig. 3a-i clearly show the details of the hydrate growth in porous media and reflect the dynamic process that the hydrate gradually fills the porous media. This experiment finds that the hydrate growth process lasts a long time, but the duration of each stage is not equal. Generally, the hydrate growth process accelerates when pressure increases. The increase in temperature shows randomness with an overall trend of increasing (Fig. 2b).

The instability period of gas–liquid dissolution: During the initial stage of the experiment, the methane gas dissolves in the aqueous solution. In this period, the metastable dissolution is transient and unconventional. Due to the low solubility and diffusion coefficient of methane gas molecules in the water, the gas–liquid contact causes a hydrophobic interaction, and the gas–liquid dissolution process shows a repeated disorder. Through observation, it can be found that the gas–liquid level in the system moves slowly. With the injection of gas, methane's enrichment degree gradually exceeds Fa solubility in water, causing the dissolution of the methane in the aqueous solution gradually stops in this period. The temperature variation diagram with the pressure changes shows that the pressure changes little in this stage, but the duration of this stage is short, about 50 s. With the injection of methane gas, the saturation of methane gas increases slowly, and the resistivity at measuring points and increase rapidly to about 4.0 Ω *m with the appearance of methane bubbles. The size of bubbles is small, with a diameter between 0.01–0.03 mm. At 50 s after the experiment began, the system's pressure and temperature begin to rise, and some methane bubbles begin to break and dissolve into the water. The gas saturation in the aqueous solution is likely to increase, which may be caused by the increase of gas-phase pressure resulted from the gas–liquid interface effect.

The hydrate growth period: With pressure increasing, the hydrate enters its growth stage. As mentioned above, when ice nuclei larger than the critical size appear in the aqueous solution, the hydrate nucleation begins, and lasts about 400 m. The ice nuclei grow spontaneously in its growth stage. At 127 s after the experiment begins, the number of bubbles begins to decrease, with the small bubbles of the early stage gather and merge. Larger bubbles appear, with a diameter of 0.1–0.5 mm, and distribute in the pores in a disperse form eventually. At 245 s after the experiment begins, the system pressure reaches 10 MPa, and the resistivity reaches about 6.0 Ω. Stop the methane gas injection at this moment, and keep observing the system for a period to ensure that the system pressure is stable at 10 MPa. Due to the dispersion-repulsion of methane gas and aqueous solution, methane gas is in a disordered state of repeated aggregation in the aqueous solution. For example, at 256 s after the experiment begins, the gas–liquid separation appears in the gas–liquid interface. At 260 s after the experiment begins, the methane bubbles break and merge at the gas–liquid interface. At 422 s after the experiment begins, the gas–liquid two phase finally becomes stable.

At 450 s after the experiment begins, a prominent stratification structure appears between the gas and the liquid. It mainly distributes in the middle of the etched glass (Fig. 3c) with the appearance of gas–liquid mixture. At 471 s after the experiment begins, a thin film forms on the surface of the hydrate which envelops the liquid phase (Fig. 3d). This phenomenon preferentially happens near the northwest of the gas source. At about 475 s after the experiment begins, the aqueous phase is completely wrapped by the hydrate film. In the meantime, the hydrate film formation ends (Fig. 3e). At 482 s after the experiment begins, the gas phase enters the aqueous phase through the hydrate in an uneven "shell-shape", and form a large amount of metastable hydrate rapidly in the aqueous phase. The resistivity of the resistance measuring point R_1 increases to 6.9 Ω *m, while the resistivity of R_2, R_3, and R_4 gradually increase to 6.8 Ω *m. The gas saturation of the liquid phase in the system reaches 33.69%. At 490 s after the experiment begins, hydrate in a more stable stage forms independently in the gas phase (Fig. 3f).

(3) The hydrate formation period: This period lasts for about 750 s, which is a relative long duration. The hydrate growth in porous media changes from disordered to ordered. The gas phase and the liquid phase change from hydrophobic to hydrophilic. During the time period of 492 s-709 s after the experiment begins, some unstable hydrates form in the liquid phase. The hydrate layer is gradually thickened, with the appearance of a great number of unstable tiny methane bubbles, but the bubble's diameter is very small. Then the system pressure continues to rise, the temperature increases to 276 K, and the methane saturation in aqueous solution further increases. At 709 s after the experiment begins, the system pressure and temperature become stable at 10.4 Mpa and 275.5 K. The gas–liquid contact stops, ice crystal structure appears, free hydrate forms in the gas phase, which proves that the methane gas and water molecules reach a stable state. The stable hydrate eventually forms, and the hydrate in free state mainly exists in the middle of the etched glass (Fig. 3g).

At 709 s after the experiment begins, the gas hydrate stops its growth, while the gas–liquid two-phase remains relatively stable, and some bright crystals appears in lumps in the pores. Influenced by the direction of the pore canal in the porous media, the crystal growth is related to the canal's direction, i.e. the crystal preferentially deposits more in the north-south channels. A large amount of hydrate is generated in the pores, but appears latter in the north-east direction (Fig. 3h). At 842 s after the experiment begins, the hydrate crystals contact with each other and aggregate, which form a hydrate layer (Fig. 3i). The hydrate stops crystallization at 1080 s after the experiment begins. A layer of stable hydrate finally forms. At this moment, the resistivity of the resistance measuring points R_1, R_2, R_3, and R_4 remain stable at 2.6–2.8 Ω *m. The hydrate saturation reaches 82.17%.

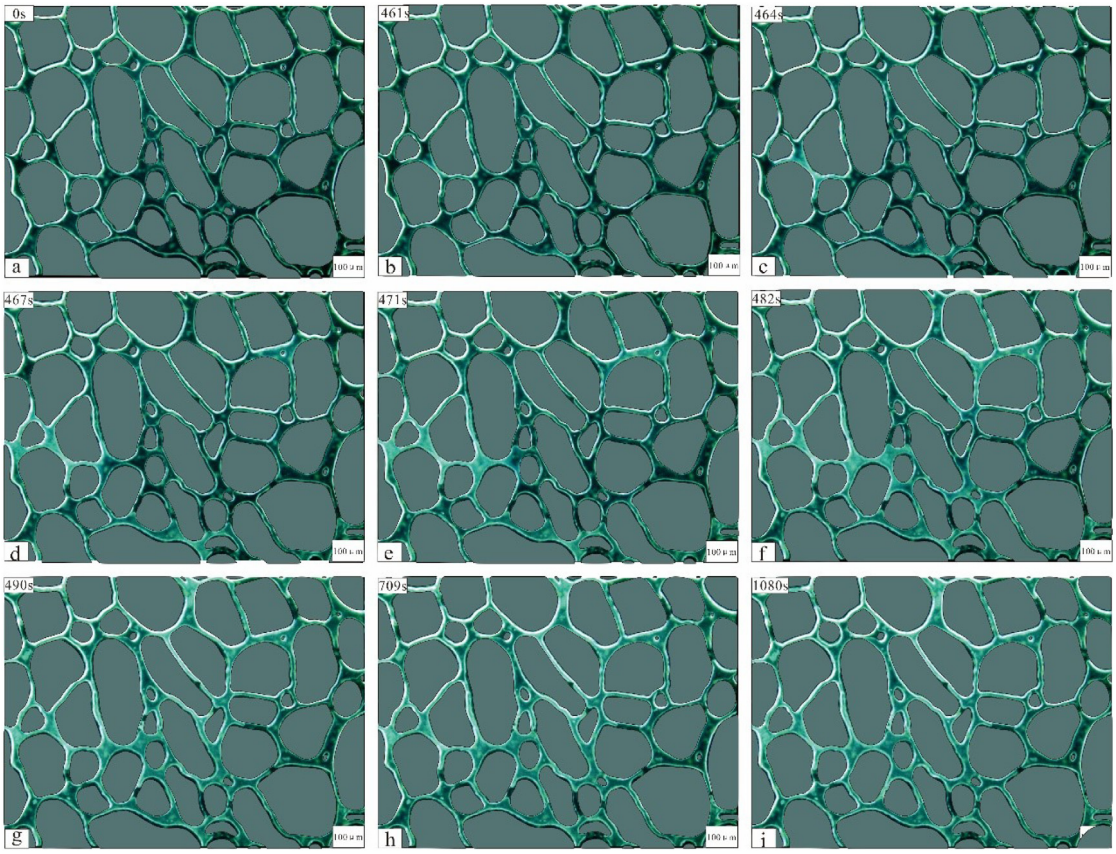

Fig. 3. Visualized hydrate formation and evolution process in micro-pore structure.

3.2. The hydrate growth mechanism

The hydrate growth period is the key stage in the whole hydrate formation process where the phase transformation happens. The hydrate's spontaneous growth has three substages: the gas–liquid cluster and nucleation stage, the gas–liquid film formation and accretion stage, and the deposition and crystallization stage. The characteristics of each stage are as follows.

3.2.1. The gas–liquid cluster and nucleation stage

Whether the hydrate nucleation happens depends on whether ice nuclei larger than the critical size appear. It is related to the hydrate's nucleation energy in the porous media (Kurihara, 2005). In this experiment, the substrate surface of the etched glass is hydrophilic, which makes the gas molecules cannot reach the porous media surface. Only when the gas and water solution exist on the substrate surface simultaneously does the nucleation happens on the substrate surface. Therefore, in general, hydrate nucleation cannot happen on the porous media surface, but preferentially happens at the gas–liquid interface.

According to the convergence process of the methane gas and the aqueous solution, the gas–liquid cluster and nucleation stage can be subdivided into two subphases: gas phase nucleation and liquid phase nucleation. Gas phase nucleation is the main incentive of the hydrate nucleation. It can be determined by the appearance of bright crystals in the gas phase, which are tiny but visible, and randomly distributed. The gas phase is dissolved in the aqueous solution in bubbles. As the gas saturation increases, the gas diffuses in the liquid phase and to the periphery of the pores. The hydrate nucleates at various positions and grows into small clusters. These small clusters contact and connect each other, which forms hydrate clusters until the ice nuclei larger than the critical size appear. As observed at 461 s after the experiment begins, free water begins to nucleate in the gas phase (Fig. 4). It is necessary to analyze the incentive mechanism of hydrate nucleation for a better explanation about the nucleation pattern (Fig. 5).

Firstly, a large amount of liquid–solid and liquid-liquid interfaces in the system. Between the gas and liquid, there is a smooth gas–liquid interface. Hydrates at the complex phase interfaces have lower free energy, which provides conditions for the formation of homogeneous nuclei. Secondly, methane gas is hydrophobic in nature, with limited solubility and low diffusion coefficient in the water phase, so the hydrate nucleation is to grow along the existing hydrate interface into the depth of the pores. In other words, new and continuous nuclei are formed on the existing heterogeneous nuclei. Comparing to an independent nucleation and growth in the pore water, this growth mode is easier and faster.

Nucleation then dominates. Hydrates nucleate at this interface and grow simultaneously into the gas and liquid phases. The clusters become larger over time, eventually forming multiple lenticular hydrate nuclei. The liquid-phase nucleation can be determined by the appearance of spontaneous accretive growth in the water phase in a closed and stable environment. The clustering and nucleation of the liquid phase are less visible, but the liquid phase nucleation can be determined by the liquid phase migration phenomenon in a stable environment. For example, the liquid phase growth can be observed at 464 s after the experiment begins (Fig. 6). It is worth mentioning that the hydrate nucleation at the interface is random. The hydrate nucleation cluster is also observed in a few pores. The reason may be the capillary-forces-driven free water migration due to the porous structure of the adjacent hydrate clusters in the formation process. The above phenomenon shows that the distribution of free water

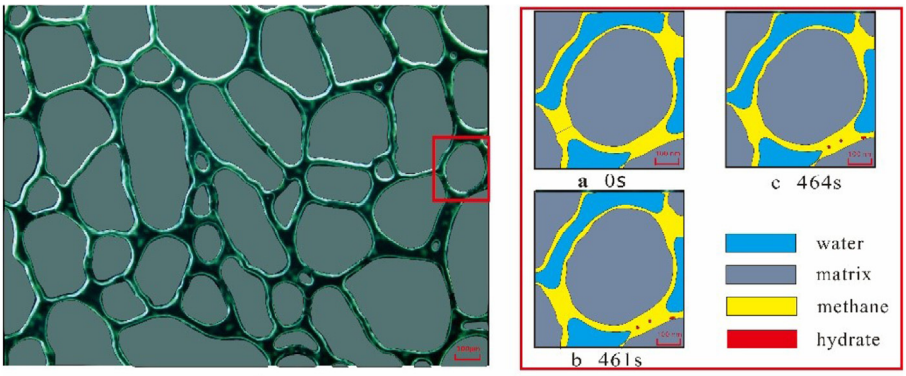

Fig. 4. Time-varying diagram of hydrate nucleation in the gas–liquid cluster and nucleation stage.

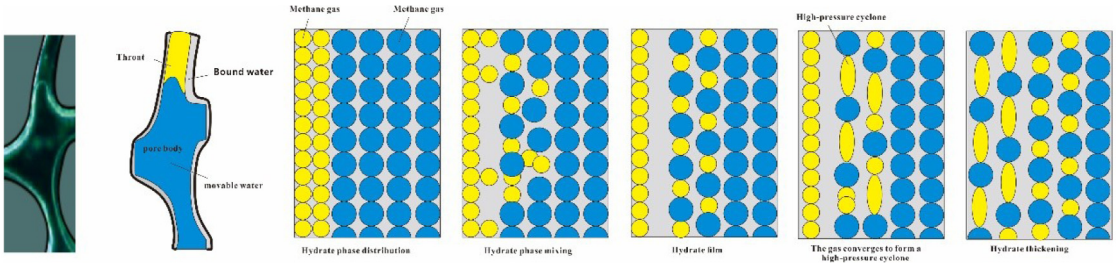

Fig. 5. Spontaneous growth model of the heterogeneous nucleation of hydrate.

largely determines the location and shape of the hydrate. Besides, water transport in the hydrate formation process also causes a considerable effect on the distribution of hydrate.

3.2.2. The gas-liquid film formation and accretion stage

The film formation stage refers to that the liquid-phase hydrate stops spontaneous nucleation, and a film-like ice crystal structure appears in the gas–liquid mixture, which can be clearly distinguished from the liquid phase. The gas–liquid film formation and accretion stage is a transition in the hydrate growth process, which can be divided into the film formation period and the accretion period according to its growth characteristics. During the hydrate film formation period, the gas phase is usually surrounded by the hydrate, which exists in "shell-shape" or "film-shape". The hydrate in these shapes hinders the transportation of gas and water at the gas–liquid interface, which leads to a slow formation of hydrates. This phenomenon is known as the "armor effect" (Yousif and Sloan, 1991). In the subsequent hydrate growth process, the hydrate film thickens (Fig. 4). Therefore, the hydrate accretion stage is also known as the hydrate thickening stage, which can be determined by a typical sign that the gas–liquid mixing stops, and the hydrate film mainly thickens at the liquid phase. In this stage, ice crystals begin to appear in the pores and gradually approaches the substrate surface. Meanwhile, free hydrates appear in the gas phase, which indicates the gas molecules' control on the formation of hydrates. The control is made by the mass transfer process that the gas molecules pass the hydrate film to the residual water. After the formation of the hydrate film, it is found that the film is formed by a large number of hydrate crystals clusters at the hydrate-methane gas interface. A great number of hollow pore structures exist on the uneven surface of the film. For example, at 482 s-490 s after the experiment begins, the hydrate thickening process becomes apparent. In the meantime, the hydrate surface becomes rough with the existence of many small pores (Fig. 7), which promotes the hydrates further grow.

In this stage, the hydrate does not contact the substrate surface directly due to a free water layer existing between in which. In other words, water holes that have not undergone phase change still exist between the hydrate clusters and the crystals. At this moment, the water phase provides support for the secondary growth of the hydrate and the formation of a skeletal structure by filling in the pores. The continuous growth of hydrates in the residual water consumes the pore water until it is exhausted, and then begins to consume the residual water. After the hydrate ultimately forms, almost no free water phase remains in the pores. Therefore, when free water is not sufficient to maintain the hydrate growth continuously, air holes form in the hydrate clusters. The hollow skeleton structure of the hydrate has limited strength and provides limited support for the particles. Therefore, it can be inferred that in where the water saturation is low, the mechanical stability of the sediment layer with hydrates will be affected.

3.2.3. The deposition and crystallization stage

The deposition and crystallization stage is a transition stage in the hydrate formation. It is apparent that in the previous stage, the hydrate thickening process lasts for a short duration, but the hydrate growth lasts for a longer duration. In the final stage of the hydrate growth, the hydrate begins to crystallize, which initially appears as the gas phase wrapping around the water phase, and preferentially forms in the pore near the north-northwest around the gas source. During the hydrate formation process, the crystals contact and aggregate with each other. The hydrates continue to grow along the surface of the particles into the small pores between the particles, until they completely fill the pores and exist in a wedge-shape (Fig. 8). The growth of hydrate crystals involves a complicated mass transfer process, which happens through a solid diffusion of water in the crystal or a diffusion along the boundary or surface of crystal, and finally forms a hydrate layer. Compared with the smooth hydrate film formed the initial stage of the hydrate formation, the hydrate crystal has

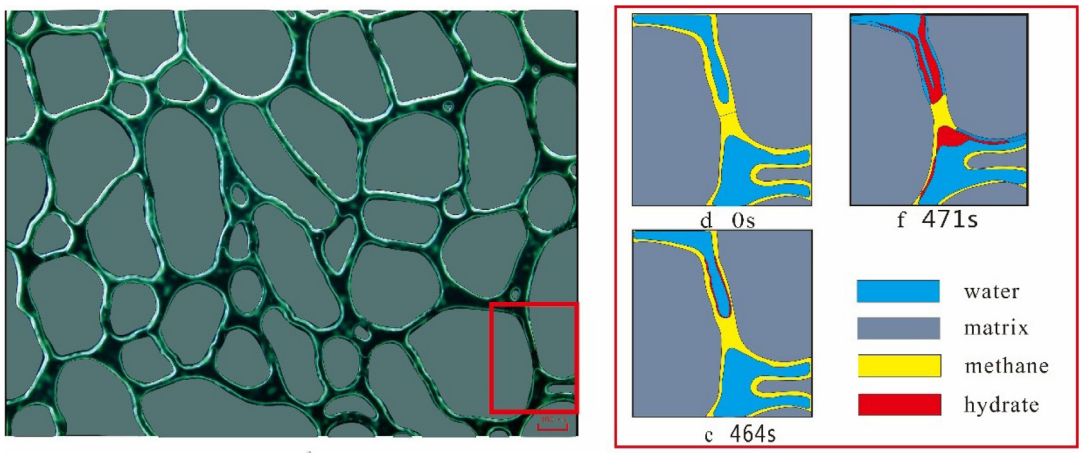

Fig. 6. Time-varying diagram of liquid-phase nucleation in the gas–liquid cluster and nucleation stage.

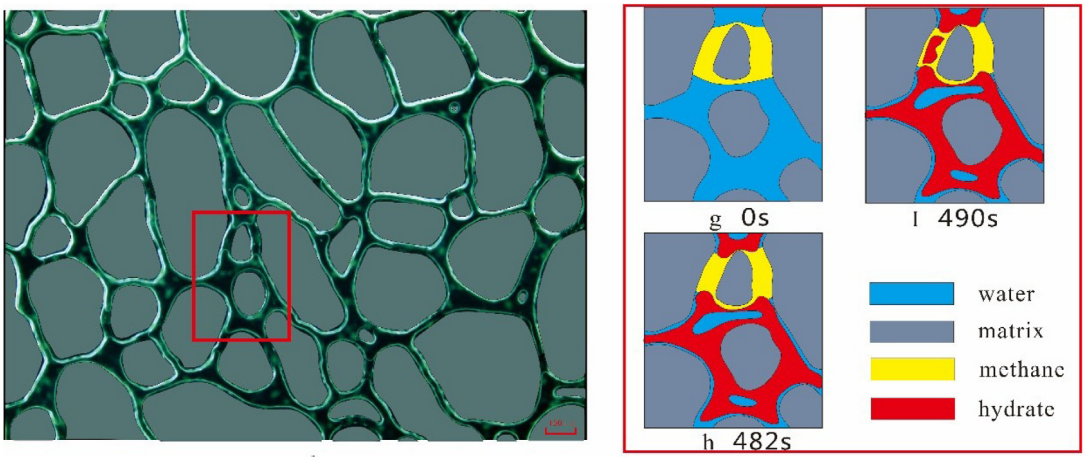

Fig. 7. Time-varying diagram of the hydrate film thickening process in the gas–liquid film formation and accretion stage.

a rougher surface and a polyhedral shape, and stretches to the liquid phase. A single polyhedron is a single hydrate crystal, which does not have a uniform size with each other. The diameter is usually between 10 and 20 μm. The boundaries of some crystals are visible. At this time, two forms of hydrates exist in the system simultaneously, namely, the hydrate who grows freely and who grows with an attachment on… As shown in Fig. 9, these two types of hydrates form and coexist between the hydrate and the substrate at 1080 s after the experiment begins.

4. Discussions

(1) The nucleation characteristics of the gas hydrate directly determine its spatial distribution in pores. According to the classical nucleation theory (Katsuki, 2008), the hydrate nucleation can be divided into two types, namely, homogeneous nucleation and heterogeneous nucleation. Homogeneous nucleation does not occur at the phase interface in the system, while heterogeneous nucleation happens at the surface of the impurities on the phase interface (including gas–liquid interface and liquid–solid interface) by forming nuclei larger than the critical size. The heterogeneous nucleation of hydrates is more complicated.

In the classical nucleation theory, the relation between the hydrate clusters' nucleation energy W (J), the clusters' structural units n, and the chemical potential difference between and the new and the old phases is as follows:

$$W(n) = -n\Delta\mu + c v_h^{2/3} \sigma_{ef} n^{2/3} \tag{7}$$

Generally, σ_{ef} is defined as (Kashchiev, 2000):

$$\sigma_{ef} = \Psi\sigma \tag{8}$$

In the above formula, is the H-dimensional nucleation energy of a single solidified phase; is the chemical potential difference between the new phase and the old phase, which is a known function of temperature T and pressure P (Kashchiev and Firoozabadi, 2002); c is the form factor of the crystal; v_h is the volume of a single structural unit of the hydrate. A structural unit includes a gas molecule and n water molecules; n is the hydration number. σ_{ef} is the effective surface energy independent of temperature and pressure; σ is the effective surface energy of the hydrate–solution interface; the factor Ψ is between 0 and 1. When the hydrate crystal completely infiltrates the substrate, $\Psi = 0$. When the hydrate does not infiltrate the substrate at all, $\Psi = 1$. Then $\sigma_{ef} = \sigma$. At this time, the hydrate homogeneous nucleation happens.

When $0<\Psi<1$,

$\sigma_{ef} < \sigma$. At this time, the hydrate heterogeneous nucleation happens.

From the above analysis, it can be seen that the homogeneous nucleation is a particular case of heterogeneous nucleation. The homogeneous nucleation forms sphere-shaped nuclei, also known as spherical cluster-shaped homogeneous nucleation. The heterogeneous nucleation forms spherical-crown-shaped nuclei, which is generally divided into two types, namely, the hat-shaped heterogeneous nucleation and the lenticular-shaped heterogeneous nucleation. Under the same external conditions, the two

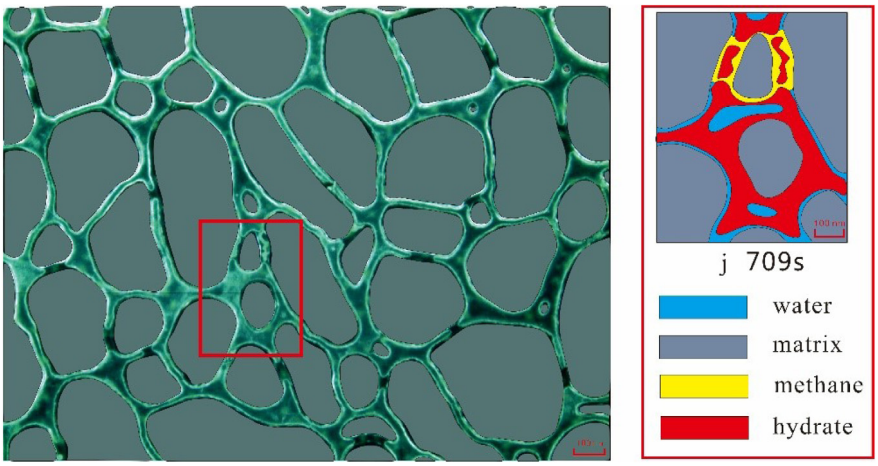

Fig. 8. Time-varying graph when the hydrate starts crystallization.

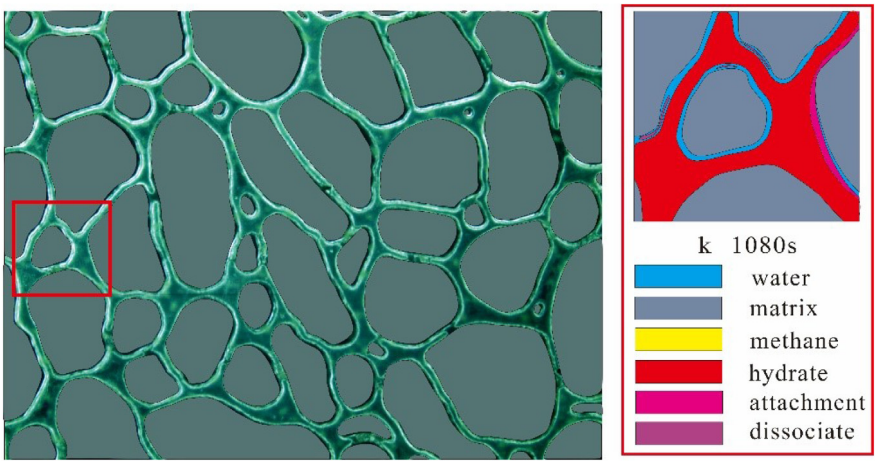

Fig. 9. Time-varying graph of the hydrate deposition and crystallization.

types have similar radii of curvature. Therefore, the occurrence rate of heterogeneous nucleation is higher than that of homogeneous nucleation. The hydrate's occurrence mode tends to be an aggregation inside the pores, rather than an adherence to the pore walls of the substrate. Furthermore, a thin layer of water always exists between the substrate and the hydrates, which makes the occurrence mode of the hydrates tend to have a suspension structure.

The hydrate growth process is an interaction of two kinds of transformations in the porous media, namely, the transformation from the disordered to the ordered, and the transformation from the hydrophobic to the hydrophilic. In the instability period of gas–liquid dissolution, due to the gas molecules' low solubility and diffusion coefficient in the water, the as-liquid contact appears to be hydrophobic, and the gas–liquid dissolution process shows a repeated disorder. During the hydrate nucleation period, the hydrate nucleation develops into a state of lower free energy. When it comes to the gas–liquid film formation and accretion stage, due to the influence of the low water saturation of the porous media, the hydrate begins to grow and spread orderly along the liquid phase, which is also known as "climbing effect". The hydrate clusters rely on the hydrate at the liquid film as the "matrix" for their continuous "reproduction" to the liquid phase. Due to their capillary forces, the hydrate growth appears as a "hydrophilic" phenomenon, which follows the existing hydrate interface to grow orderly into the depth of the pores.

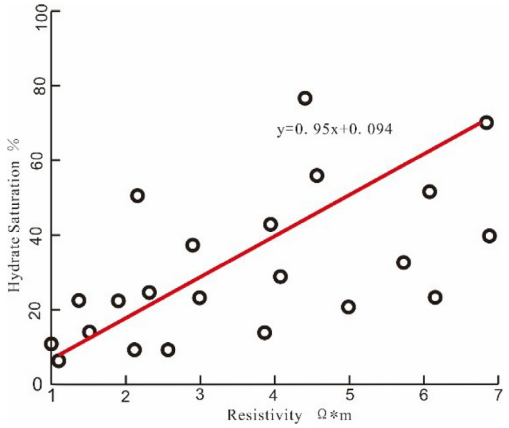

Fig. 10. Correlation curve between resistivity and saturation.

(3) The growth of the hydrates is a circuitous process. It has a significant impact on the permeability, resistivity, and the saturation of the porous media. The in-situ resistivity and the gas saturation of the hydrates increase, while the permeability decreases. In general, the resistivity and the saturation are positively correlated (Fig. 10). In different stages, the growth rate of the hydrate has a segmented growth feature, which is generally

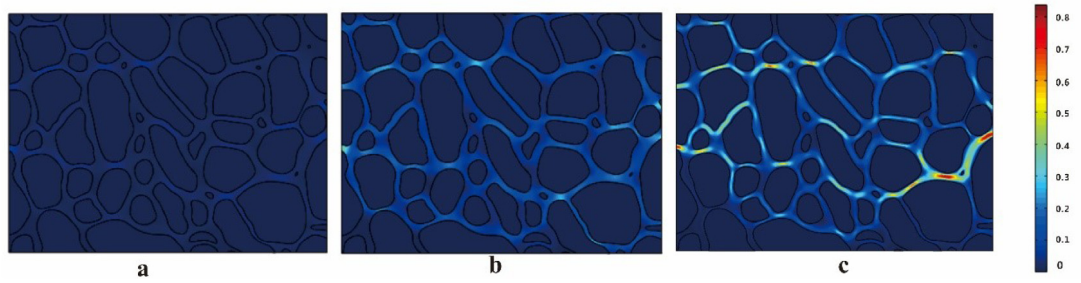

Fig. 11. Hydrate growth and evolution figure in three periods based on comsol liquid simulation method.

slow at first and then fast (Fig. 2c). The hydrate growth is slow during the nucleation and accretion stage, but increases rapidly after the end of the accretion stage. For instance, at 780 s after the experiment begins, the hydrate growth accelerates sharply. As the gas saturation of the hydrate increases, the permeability in the pores gradually decreases, and the change in permeability in the pore space hinders the liquid from flowing in the pores. It further causes a temporary stagnancy in the hydrate growth, reduces the hydrate growth rate, and increases the hydrate resistivity. At 850 s, 864 s and 912 s after the experiment begins, the growth rate fluctuates transiently.

(4) The geometric distribution of the pore structure can change the spatial structure of the water molecules' growth, which leads the hydrate to distribute with a geometric anisotropy. The experiment results show that: 1) The hydrate growth rate is faster at the position closer to the gas source. For example, in the etched glass, the hydrate near the gas source forms preferentially, while the hydrate growth in the position far from the gas source lasts for a longer time. 2) When the pore throat's direction is similar to the transport direction of the methane gas, the hydrate growth rate is better than the pore throats with other directions. For instance, the hydrate growth rate and the hydrate nucleation rate in NW and NNW direction are faster than that in NE direction. In order to verify this conclusion, this experiment uses a liquid simulation method to analyze the dynamic process of the hydrate growth in porous media. It can be seen from the Hydrate Growth and Evolution Diagram (Fig. 11) that the hydrate synthesis rate in the pore canal is different in different synthesis periods. In general, the hydrate growth shows a strong heterogeneity characteristic. In other words, the hydrate growth rate is closely related to the gas source's position and the pore throat's direction. The hydrate first forms in the area near the gas source, and the pore throats in the same direction with the gas injection direction. These facts effectively verify the above conclusions.

5. Conclusion

(1) The hydrate formation and evolution are divided into three periods, including the instability period of gas–liquid dissolution, the hydrate growth period, and the hydrate formation period. Hydrate's nucleation and spontaneous growth occur in the hydrate growth period. The hydrate growth period has three substages: the gas–liquid cluster and nucleation stage, the gas–liquid film formation and accretion stage, and the deposition and crystallization stage. In different periods and stages, the characteristics of the hydrate growth differ significantly.

(2) The nucleation characteristics of the gas hydrate directly determine the hydrate's spatial distribution in the pores. The heterogeneous nucleation is more likely to occur. The hydrate preferentially forms at the gas-water interface, where the hydrate film thickens toward the liquid phase as the reaction going on, and gradually approaches the rock matrix. The gas diffusion and mass transfer happen through the porous hydrate layer to the aqueous phase. The occurrence mode of the hydrate is more like a suspension structure.

(3) The spatiotemporal growth of the hydrates is an interaction of two kinds of transformations in the porous media, namely, the transformation from the disordered to the ordered, and the transformation from the hydrophobic to the hydrophilic. Affected by the lower solubility and diffusion coefficient of gas molecules in water, in the early stage, the gas–liquid contact appears to be hydrophobic, and the gas–liquid dissolution process shows a repeated disorder. In the later stage, due to the influence of the low water saturation of the porous media, the hydrate begins to be "hydrophilic", which means it follows the existing hydrate interface to grow orderly into the depth of the pores.

(4) The growth of the hydrate is a circuitous process, and has a significant impact on the permeability, resistivity, and the hydrate saturation of the porous media. In general, the in-situ resistivity and the gas saturation of the hydrates increase, while the permeability decreases. The resistivity and the saturation are generally positively correlated.

(5) The geometric distribution of the pore structure can change the spatial structure of the water molecules' growth, which leads the hydrate to distribute with a geometric anisotropy. The hydrate growth rate is faster at the position closer to the gas source. When the pore throat's direction is similar to the transport direction of the methane gas, the hydrate growth rate is better than the pore throats with other directions.

Declaration of competing interest

The authors declare that they have no known competing financial interests or personal relationships that could have appeared to influence the work reported in this paper.

CRediT authorship contribution statement

Dian-ju Wang: Investigation.

References

Kashchiev, D., 2000. Nucleation: Basic Theory with Applications. Butterworth-Heinemann, Oxford.

Kashchiev, D., Firoozabadi, A., 2002. Nucleation of gas hydrates. J. Cryst. Growth 243, 476–489.

Katsuki, D., 2008. Visual observation of dissociation of methane hydrate crystals in a glass micro model : Production and transfer of methane. J. Appl. Phys. 104 (8), 083514-083514-9.

Kurihara, M., 2005. Investigation on applicability of methane hydrate production methods to reservoirs with diverse characteristics. In: International Conference on Gas Hydrate, Trondheim.

Lu, H., Hu, G., Vanderveen, J., et al., 2011. Factors Affecting the Process of CO2 Replacement of CH4 from Methane Hydrate in Sediments - Constrained from Experimental Results. American Geophysical Union.

National Energy Technology Laboratory of U.S. Department of Energy, 1999-2016. The U.S. Methane Hydrate R & D Program. Research Publications and Presentations of DOE Supported Methane Hydrate R & D 1999-2016.

Ota, M., Abe, Y., Watanabe, M., et al., 2005. Methane recovery from methane hydrate using pressurized CO2. Fluid Phase Equilib. 228, 553–559.
Sloan, E.D., 1998. Clathrate Hydrates of Natural Gases, second ed. Marcel Dekker, New York, pp. 457–460.
Wan, Yizhao, Wu, Nengyou, Hu, Gaowei, et al., 0000. Reservoir stability in the process of natural gas hydrate production by depressuriza-tion in the Shenhu area of the South China Sea. Natur. Gas Ind. 38 (4), 117–128. (in Chinese).
Xu, C., Li, X., 2015. Research progress on methane production from natural gas hydrates. Cheminform 46, 54672–54699.
Yousif, M.H., Sloan, E.D., 1991. Experimental investigation of hydrate formation and dissociation in consolidated porous media. SPE Reserv. Eng. 6, 452–458.
Zhou, X., Fan, S., Liang, D., et al., 2008. Replacement of methane from quartz sand-bearing hydrate with carbon dioxide-in-water emulsion. Energy Fuels 22, 1759–1764.
Zunzhao, L.I., Guo, X., Chen, G., et al., 2007. Experimental and kinetic studies on methane replacement from methane hydrate formed in SDS system by using pressurized CO2. J. Chem. Indu. Eng. 58, 1197–1203.